



## ORIGINAL ARTICLE

# Investigation of the anisotropic mechanical response of layered shales

Min Gao<sup>1,2</sup> | Bin Gong<sup>3</sup>  | Zhengzhao Liang<sup>4</sup> | Shanpo Jia<sup>2</sup>  | Jiuqun Zou<sup>1</sup>

<sup>1</sup>Engineering Research Center of Underground Mine Construction (Chinese Ministry of Education), Anhui University of Science and Technology, Huainan, China

<sup>2</sup>School of Earth Science, Northeast Petroleum University, Daqing, China

<sup>3</sup>Department of Civil and Environmental Engineering, Brunel University London, London, UK

<sup>4</sup>State Key Laboratory of Coastal and Offshore Engineering, Dalian University of Technology, Dalian, China

## Correspondence

Bin Gong, Department of Civil and Environmental Engineering, Brunel University London, London UB8 3PH, UK.  
Email: [bin.gong@brunel.ac.uk](mailto:bin.gong@brunel.ac.uk)

## Funding information

Engineering Research Center of Underground Mine Construction, Chinese Ministry of Education, Grant/Award Number: JYBGCZX2022108; Natural Science Foundation of Anhui Province, Grant/Award Number: 2108085QE208; Anhui University, Grant/Award Number: 2022AH050798; China Postdoctoral Science Foundation, Grant/Award Number: 2021M700753; University Synergy Innovation Programme of Anhui Province, Grant/Award Number: GXXT-2022-20

## Abstract

Layered shales exist widely and are often encountered during shale gas development. However, the mechanical response of layered shales is significantly affected by the existence of beddings, resulting in the obvious anisotropy characteristics regarding deformation, strength and failure mode. To clarify the underlying mechanisms of shale anisotropy that control the safety of engineering projects, the numerical simulation and theoretical analysis were conducted. The results show that with the growth of confining pressure, the compressive resistance of shales gradually increases, the shear fractures govern the instability and the anisotropy index decreases. Furthermore, several strength criteria for layered rock masses were summarized, and the modified Jaeger strength criterion was proposed by introducing the anisotropic parameter  $R_{c\phi}$ . It can effectively reflect the failure modes and strength features of layered shales under triaxial conditions with a higher accuracy. Besides, the variation of cohesion and internal friction angle of layered shale samples was comprehensively analysed under the triaxial conditions. Clearly, as the inclination angle of bedding planes increases, the cohesion of layered shales first decreases, but then increases under triaxial compression, showing the 'U'-shaped changing trend. Additionally, the internal friction angle of layered shales gradually increases with the increase in the inclination of bedding planes.

## KEYWORDS

anisotropy, failure criterion, layered shales, shale gas development, triaxial compression

# 1 | INTRODUCTION

Anisotropy is a critical mechanical characteristic of layered shales and has raised much attention of geotechnical engineers for shale gas exploration and development. Generally, metamorphic rocks (e.g., slate, gneiss and phyllite) and sedimentary rocks (e.g., shale) are sensitive to the structural anisotropy and behave differently along various directions. Actually, the influence of the pre-existing discontinuities on the mechanical behaviour of shales cannot be ignored.<sup>1,2</sup> In recent years, some researchers have investigated the anisotropic properties of layered rock masses under compression. For example, Wang et al.<sup>3</sup> proposed an elastoplastic model for layered rock mass that exhibited hybrid initial and stress-induced anisotropy. By taking shale as the research object, the anisotropic characteristics of the strength, deformation and failure mode of shales under uniaxial and triaxial compression conditions were discussed and a calculation method for evaluating the shale brittleness index was proposed. Meanwhile, three main failure types were summarized, that is, vertical tension-splitting failure, shear-slip failure along weak bedding plane and shear failure passing shear bedding plane. At the same time, with increasing confining pressure, the anisotropy of rock strength will be gradually weakened.<sup>4–7</sup> Simultaneously, the triaxial loading and unloading tests were carried out on shales, and the mechanical response, deformation characteristics and damage evolutions of Longmaxi shale were investigated.<sup>8</sup> Jin et al.<sup>9</sup> also evaluated the deformation, strength and fracture properties of Marcellus shales through laboratory tests. They pointed out that the transverse isotropic model can describe the elastic properties of Marcellus shales under compression and pure tension, and the fracture properties of Marcellus shales are anisotropic. Yang et al.<sup>10</sup> tested the typical anisotropic mechanical properties and brittleness of Longmaxi shales under conventional triaxial compression and proposed a new brittleness index to evaluate the shales with different failure modes. Mandal et al.<sup>11</sup> performed the constant rate multistage triaxial tests on Goldwyer gas shale formation, and the anisotropy of elastic and mechanical properties of shales was analysed. However, the influence mechanisms of the continuous initiation and propagation of microcracks on fracture-induced shale anisotropy remain unclear.

Furthermore, by taking layered sandstone or slate as the research object, the influence of the bedding plane orientation on their mechanical properties and failure modes was analysed in detail through laboratory tests.<sup>12</sup> The results showed that the elastic modulus, compressive strength, cohesion and friction angle first decreased and

then increased, showing a ‘U’-shaped curve. For different types of sandstones, the elastic modulus varied with the inclination angle of the bedding planes changing and is not always consistent. Basically, it can be divided into two categories: the first one is that the elastic modulus increases with the bedding orientation rising, and the other one is that the elastic modulus first increases and then decreases as the bedding orientation rises, which is similar to the variation of compression strength. The failure mode of the layered sandstone under uniaxial compression is similar to the shale, which can be divided into split-tension failure, shear-slip failure along the bedding weak plane and compression shear failure. Liao et al.<sup>13</sup> investigated a high-temperature conventional triaxial compression test on layered sandstone, and the variation in the deformation parameters, strength characteristics and failure mode of the samples with changing temperature and bedding angle was analysed and the temperature effect of the layered sandstone anisotropy was studied. Li et al.<sup>14</sup> carried out the shock compression and shock splitting tensile tests on five sample groups of layered sandstones with different bedding plane dip angles using a separate Hopkinson pressure bar test platform to analyse the effect of bedding plane dip angles on the dynamic stress–strain, dynamic influence law of compressive tensile strength, failure mode and energy absorption properties. Li et al.<sup>15</sup> performed the uniaxial compression and Brazilian splitting tests on Silurian silty slate. The mechanical properties, anisotropy characteristics and deformation failure modes of the samples were analysed, and the mechanical mechanisms of different failure modes were revealed. The existence of the silty slate surface makes the silty slate show obvious anisotropy. The main failure modes of the silty slate can be divided into two types, that is, tension-splitting failure and shear failure along the slab surface. Gholami and Rasouli<sup>16</sup> performed the laboratory experiments on the dry and wet slate samples with different bedding plane inclination angles, and the anisotropic characteristics of slate strength were analysed. When the bedding orientation is between 30° and 40°, the stiffness of the specimen will decrease, and for the wet slate specimen, the stiffness reduction is more pronounced.

Besides, Tien and Tsao<sup>17</sup> used similar materials to simulate layered rock masses and conducted relevant laboratory experiments. Using a rotary scanning instrument, they obtained the tiled images of the samples under different stress levels in the uniaxial compression test and divided the failure modes into sliding failure and nonsliding failure along the discontinuous surfaces. Then, the calculation approach of transverse isotropy parameters was determined through theoretical analysis. Moreover, the failure criterion of a transverse isotropic

rock mass proposed by Nova-Sacchi was verified by a triaxial compression test of a layered rock mass, and the calculation method of the failure surface under compression of a layered rock mass was given by theoretical analysis.<sup>18</sup> Hakala et al.<sup>19</sup> investigated the transverse isotropic mechanical properties of rocks in the Kiroto area of Finland and pointed out that the high anisotropy coefficient will lead to the obvious errors in the measurement of in situ stress. Zhou et al.<sup>20</sup> carried out a series of uniaxial and triaxial compression tests on on-site layered rock mass samples, and the related deformation behaviour and failure mode were deeply studied. Simultaneously, the layered rock mass can be usually regarded as a transversely isotropic rock material with five elastic constants. Wang et al.<sup>21</sup> theoretically studied the effective moduli of anisotropic rocks based on the Kuster-Toksöz and Mori-Tanaka models. Dambly et al.<sup>22</sup> proposed a direct method for determining the shear modulus of transversely isotropic rocks based on the uniaxial compression test of cylindrical specimens. Gonzaga et al.<sup>23</sup> carried out a hydrostatic compression test and uniaxial compression test on the standard cylindrical specimens, and a method for determining the linear elastic mechanical parameters of transversely isotropic rock was proposed. The anisotropic properties of deformation and strength of gneiss, shale and schist with different bedding plane angles were studied by uniaxial compression and Brazilian splitting tests, and a multistrain test method was proposed to determine five independent elastic parameters of transversely isotropic rocks.<sup>24</sup> Togashi et al.<sup>25,26</sup> conducted a triaxial compression test on a single transversely isotropic rock sample with varying bedding plane angles and proposed a method for determining the anisotropic elastic parameters of the transversely isotropic rock mass.

In terms of numerical simulation, Debecker and Vervoort<sup>27</sup> modelled the anisotropic strength of slate and analysed the failure modes under uniaxial compression and Brazilian splitting tests using the two-dimensional (2D) discrete element method (DEM).<sup>28</sup> This model simulated the fracture process of seven kinds of layered rock samples with different bedding plane inclination angles under uniaxial compression using the 2D rock failure process analysis (RFPA) method, and the strength, failure mode and failure criteria of the samples were discussed. Xia et al.<sup>29</sup> established a mesoscopic numerical model of a layered rock mass by the particle flow method, and the effects of bonding strength, friction and occlusion on the strength of layered rock mass were analysed from a mesoscopic perspective. The basic algorithm of the 2D discontinuous displacement method for simulating transversely isotropic elastic materials was developed and verified by the theoretical

solutions and finite element solutions.<sup>30</sup> Park et al.<sup>31</sup> proposed the bonded particle DEM method. The anisotropic mechanical properties of transversely isotropic rocks were simulated and verified by a series of laboratory tests. On this basis, a three-dimensional (3D) bonded particle DEM method was further proposed, which can accurately describe the variation law of the rock elastic modulus and strength with the bedding plane dip changing. The transverse isotropic elastic model was also embedded into the Y-Geo finite element-discrete element programme and the corresponding numerical simulations were carried out to study the progressive failure process of layered rocks and the anisotropic deformation and strength indices.<sup>32</sup> Although many related studies have been carried out to capture the anisotropic mechanical properties of different types of layered rock masses by means of laboratory tests, numerical simulations and theoretical analyses, both the understanding of underlying mechanical mechanisms and the effective methods for determining the anisotropic deformation and strength parameters of layered shales are still limited because of the influence of the creation and evolution of microcracks.

In this study, to clarify the effect mechanisms of bedding plane orientation on the anisotropic deformation and strength parameters of layered shales, systemic numerical simulations and theoretical analyses were conducted. On one hand, the progressive failure process of layered shales was modelled based on the statistical strength theory, damage mechanics and continuum theory, and the influence of the formation and development of microcracks on the mechanical resistance and failure mode of layered shales was comprehensively investigated. On the other hand, several strength criteria for layered rock masses were compared, and the modified Jaeger strength criterion was proposed by introducing the anisotropic parameter  $R_{co}$ . It can effectively reflect the failure modes and strength features of layered shales under triaxial conditions with a higher accuracy. In addition, the variation of cohesion and internal friction angle of layered shale samples was comprehensively analysed under the triaxial conditions.

## 2 | METHODOLOGY

### 2.1 | Theoretical principles

The numerical simulations of the layered shale samples under uniaxial and triaxial compression were carried out using the RFPA method<sup>33-35</sup> based on the statistical strength theory, damage mechanics and continuum theory. By introducing the heterogeneity coefficient to

characterize the heterogeneity of rock material, it can simulate the redistribution of the stress field and the induced creation and evolution of microfractures.<sup>36–38</sup> It has been applied to numerically reproduce the gradual failure process of rock material by many researchers.<sup>39–41</sup> Compared with the traditional finite element method, the RFPA method has three main characteristics: (I) The heterogeneity of rock material can be considered, and the nonlinear deformation and failure process of rock material can be simulated on the basis of the elasto-brittle-plastic constitutive model. (II) Each representative volume element will maintain the linear deformation state until the element stress satisfies the strength criterion. The element still has a certain residual strength after failure, but the element stiffness will gradually decrease. In this way, RFPA can simulate the strain softening of rock materials and the discontinuous problems based on the continuum mechanics. (III) The maximum tensile stress and maximum tensile strain criteria are used in the RFPA method. The maximum tensile stress criterion can predict brittle failure from the elastic stage to the residual deformation stage, and the maximum tensile strain criterion is used to predict the state when the element completely loses its bearing capacity.

To reflect the heterogeneity, the random distribution state of material properties on the element level can be characterized by introducing the Weibull distribution function,<sup>42</sup> and its function expression is

$$\varphi = \frac{m}{\sigma_0} \left( \frac{\sigma}{\sigma_0} \right)^{m-1} \exp \left[ - \left( \frac{\sigma}{\sigma_0} \right)^m \right], \quad (1)$$

where  $\sigma$  is the element strength,  $\sigma_0$  is the mean strength of all elements of the sample, and  $m$  is the heterogeneity coefficient.

## 2.2 | Numerical models

Figure 1 displays the load conditions of a layered shale sample, where  $\theta$  is the inclination angle of the bedding planes, that is, the angle between the loading direction and the normal direction of the bedding planes, and  $\theta_m$  is the angle between the loading direction and the bedding planes ( $\theta + \theta_m = 90^\circ$ ). Then, the numerical shale samples with different bedding plane dip angles were established in the RFPA<sup>3D</sup> code, as shown in Figure 2. The samples were composed of both rock material and bedding surface material with a size of 50mm × 50mm × 100mm and a bedding plane spacing of 2mm. The displacement-controlled loading mode was adopted, and the loading rate was 0.005mm/step. In the

numerical simulation, the confining pressure was set to be 2, 5, 10 and 15 MPa to investigate the deformation and failure law of layered shales under triaxial compression.

## 2.3 | Physical experiment and model parameter calibration

To determine the mechanical parameters of the layered shales, seven shale samples with different bedding dip angles were loaded in the uniaxial compression test, as shown in Figure 3. The rock mechanics test system RMT-150C as shown in Figure 4 was used to perform the experiments. It was made by the Institute of Rock and Soil Mechanics, Chinese Academy of Science, China. The RMT-150C is featured by complete test functions, easy operation and a high degree of automation. Meanwhile, tests can be completely controlled by the computer. During the tests, the operator can intervene by changing the control mode and test parameters. The test steps can also be set in advance and completed automatically by the computer. At the end of the test, the system can automatically return to the initial state and can easily generate the test results. The displacement loading mode was adopted in this test and the loading rate was 0.0005mm/s. Meanwhile, an LVDT deformation sensor was used to measure the axial and lateral deformation.

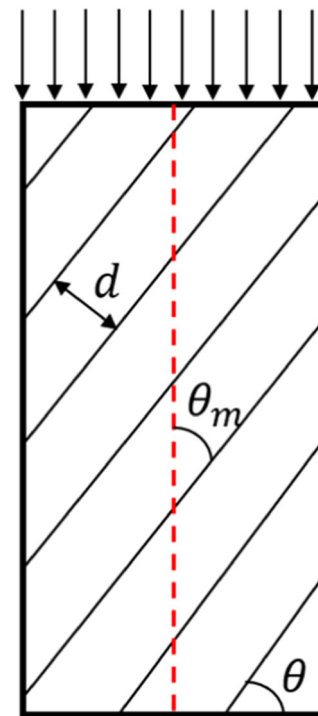


FIGURE 1 Load diagram of the layered shales.



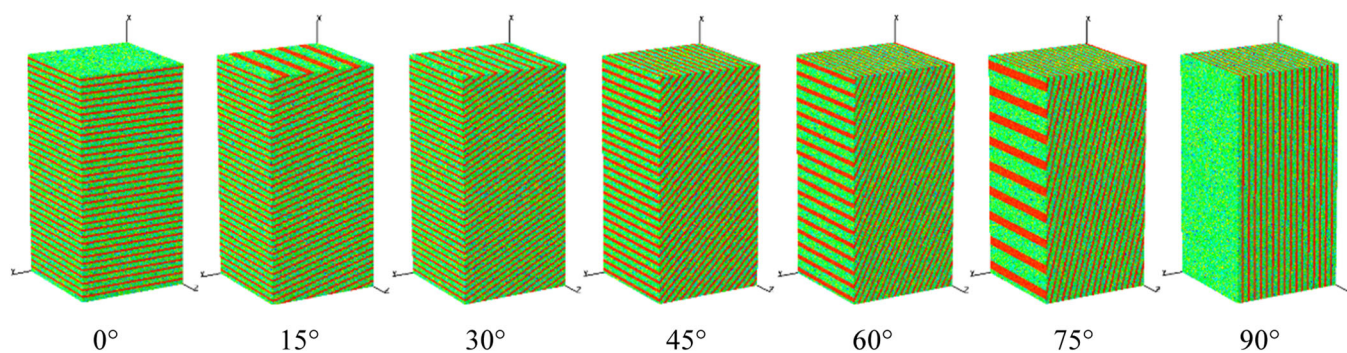


FIGURE 2 Numerical models of the layered shales with different inclination angles.

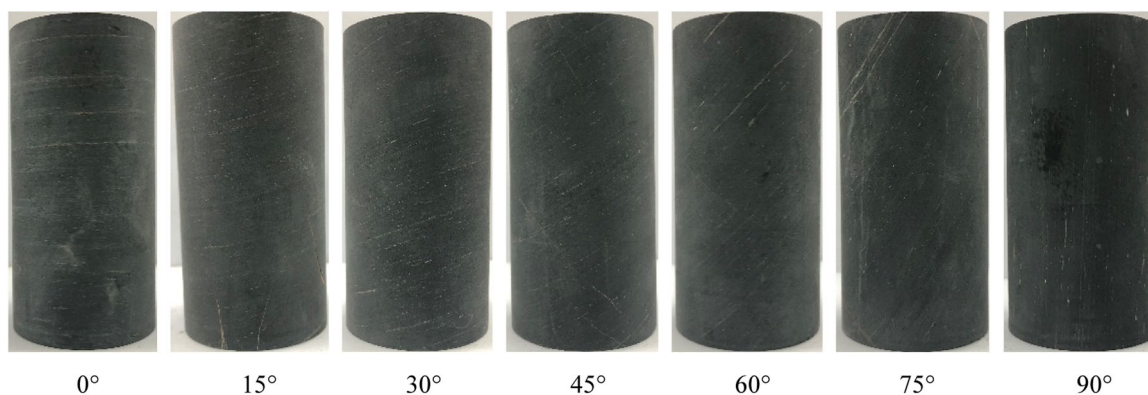


FIGURE 3 Layered shale samples with different bedding orientations.



FIGURE 4 RMT-150C rock mechanics testing machine.

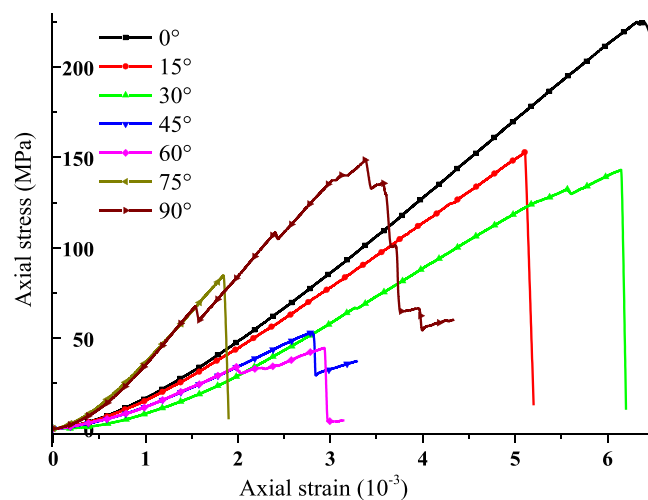


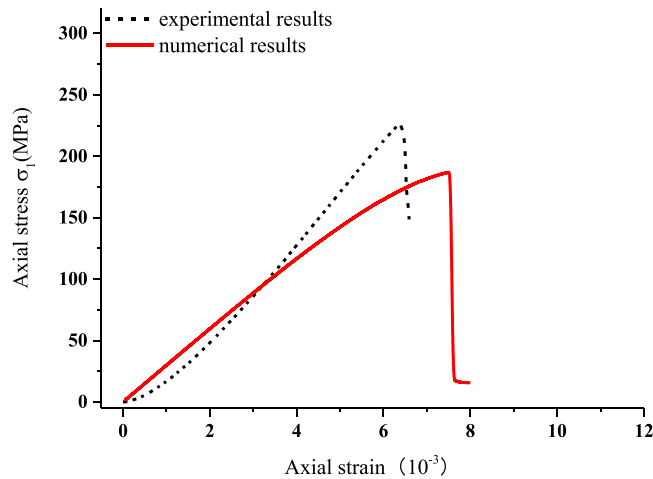
FIGURE 5 The stress-strain curves of the shale samples under uniaxial compression.

Figure 5 shows the compressive stress-strain curves of the shale samples with different bedding dip angle from which we can see that before the peak strength, the axial stress basically increases linearly

with the axial strain rising, and the lateral strain is smaller than the corresponding axial strain value. After reaching the peak strength, the lateral strain value suddenly increases, indicating that the shale samples

**TABLE 1** Mechanical parameters of the layered rocks for simulation.

Material	Compressive strength (MPa)	Elastic modulus (MPa)	Poisson's ratio	Heterogeneity coefficient
Rock	230	13,000	0.18	4
Bedding plane	23	1300	0.20	3

**FIGURE 6** Comparison of experimental results and numerical results of a sample with 0°.

have strong brittle characteristics. For the bedding plane orientation between 60° and 90°, there is a stress drop in the stress–strain curve before reaching the peak strength, which is mainly caused by the cracking of the bedding surfaces inside the sample. As the axial load continues to increase, the critical parts of the bedding surfaces and rock media are damaged, causing the overall failure of the samples. Compared with the other samples, the stress drop in the postpeak stress–strain curve of the sample with a bedding orientation of 90°, is relatively slow, and there is a phenomenon of progressive failure. At the same time, it can be seen from the stress–strain curves that the uniaxial compressive strength reaches the minimum value (44.68 MPa) when the bedding orientation is 60° and reaches the maximum value (225.22 MPa) when the bedding orientation is 0°.

The triaxial compression numerical model was composed of two materials, that is, rock matrix and bedding plane. According to the experimental results and related references, the uniaxial compressive strength, elastic modulus, Poisson's ratio and heterogeneity coefficient of two materials were determined for simulation, as shown in Table 1. The stress–strain curve calculated by the numerical simulation were also compared with the test data as shown in Figure 6, which proves the effectiveness and rationality of the chosen parameters.

### 3 | MICROCRACK AFFECTED ANISOTROPY OF LAYERED SHALES

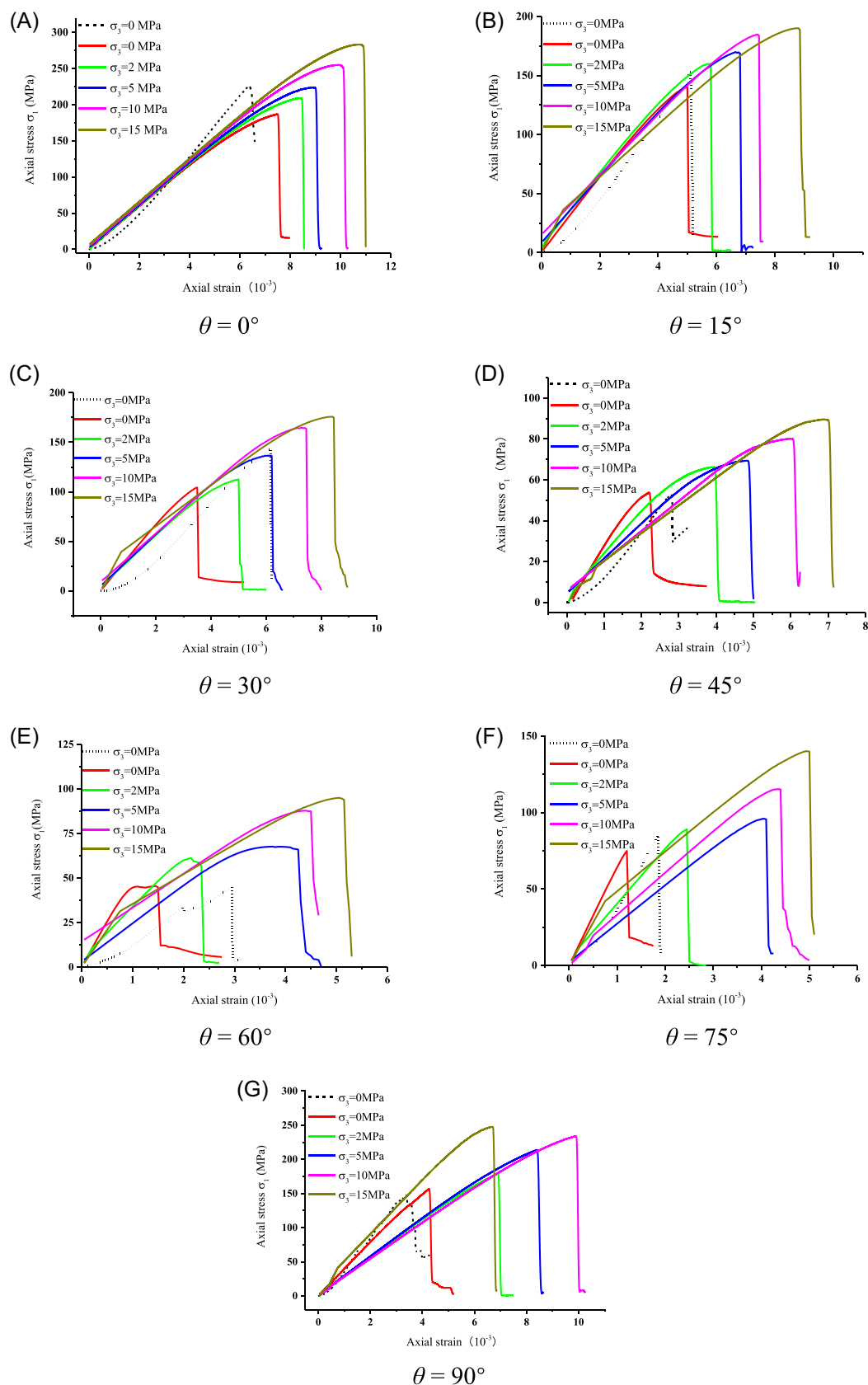
#### 3.1 | Stress–strain curve analysis

Figure 7 shows the axial stress–strain curves of the layered shale samples under different confining pressures. The black dashed curve represents the uniaxial compression chamber test results ( $\sigma_3 = 0$  MPa). It can be seen from Figure 7 that the confining pressure has a significant effect on the strength of the layered rock mass samples. For the layered shales with the same dip angle, the axial peak strength increases with the growth of the confining pressure. Simultaneously, with the confining pressure increasing, the plastic deformation stage before the peak of the axial stress–strain curve is more obvious, and the layered rock samples with different dip angles gradually change from brittle failure to plastic failure.

Figure 8 shows the axial stress–strain curves of the layered shale samples with different dip angles. According to the stress–strain curves of the samples under different confining pressures, the mechanical characteristics of the samples with different dip angles are obviously different. The failure strength and elastic modulus of the samples are greatly affected by the inclination of the bedding planes, meaning that the mechanical characteristics of the layered rock samples have significant anisotropy. According to the stress–strain curves, it can also be found that the stress drops rapidly after the sample reaches the peak strength, indicating that the sample has a strong brittle characteristic. When the confining pressure is 5 or 10 MPa, the brittleness characteristic of the specimens with the bedding orientations of 30° or 60° are slightly weaker than the other specimens. This reveals that the brittle characteristic of the layered rock samples is also anisotropic.

#### 3.2 | Strength and deformation characteristics

According to the stress–strain curves in Figures 7 and 8, the strength, axial strain and elastic modulus at the peak point of the layered shales with different dip angles can be obtained, as shown in Figure 9. The black dotted line in Figure 9 shows the experimental results. Figure 9A



**FIGURE 7** Axial stress–strain curves of the layered shale specimens under different confining pressures when: (A)  $\theta = 0^\circ$ , (B)  $\theta = 15^\circ$ , (C)  $\theta = 30^\circ$ , (D)  $\theta = 45^\circ$ , (E)  $\theta = 60^\circ$ , (F)  $\theta = 75^\circ$  and (G)  $\theta = 90^\circ$ .

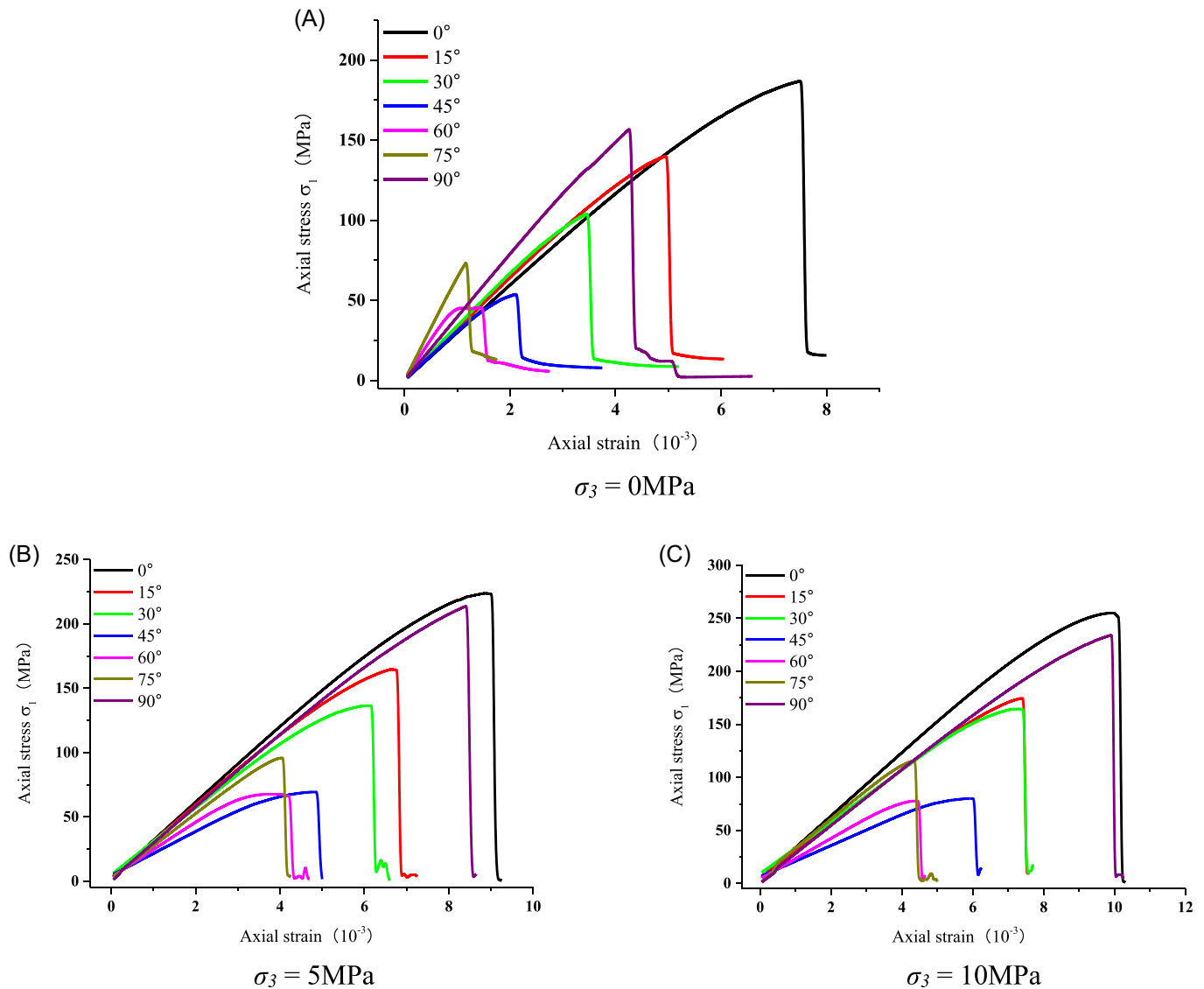


**FIGURE 8** Axial stress–strain curves of the layered shale specimens with different bedding inclinations when: (A)  $\sigma_3 = 0$  MPa, (B)  $\sigma_3 = 5$  MPa and (C)  $\sigma_3 = 10$  MPa.

illustrates that with an increase in the inclination angle of the bedding plane, the peak compressive strength of the layered rock mass first decreases and then increases, showing a typical ‘U’-shaped variation. For the layered rock samples with the same orientation, the peak strength of the sample increases gradually with an increase in the confining pressure. Furthermore, when the bedding plane inclination is 0°, the peak intensity of the sample is the largest, and when the inclination of the bedding plane is 45° or 60°, the peak intensity of the sample is the smallest. Figure 9B displays the corresponding axial strain at the peak strength. It can be seen that with the inclination angle of the bedding planes rising, the variation in the axial strain value at the peak point is similar to the peak strength, that is, typical ‘U’-shaped changing trend. When the confining pressure is 2 MPa, the strain value at the peak point

fluctuates slightly, but the overall variation law is consistent with the other confining pressures. Figure 9C shows the variation curve of the elastic modulus with the inclination angle of the bedding plane changing. Basically, with the inclination angle of the bedding plane increasing, the elastic modulus first decreases, later increases and then decreases, similar to the ‘W’-shaped curve. When the inclination of the bedding plane is 30° or 75°, the elastic modulus has a peak point, and the elastic modulus reaches the minimum value when the bedding plane inclination angle is 45°. The comparison between the uniaxial compression test results and the numerical simulation results in Figure 9 shows that the compressive strength, the axial strain at the peak point and the elastic modulus are nearly consistent, proving the validity and rationality of the simulations.



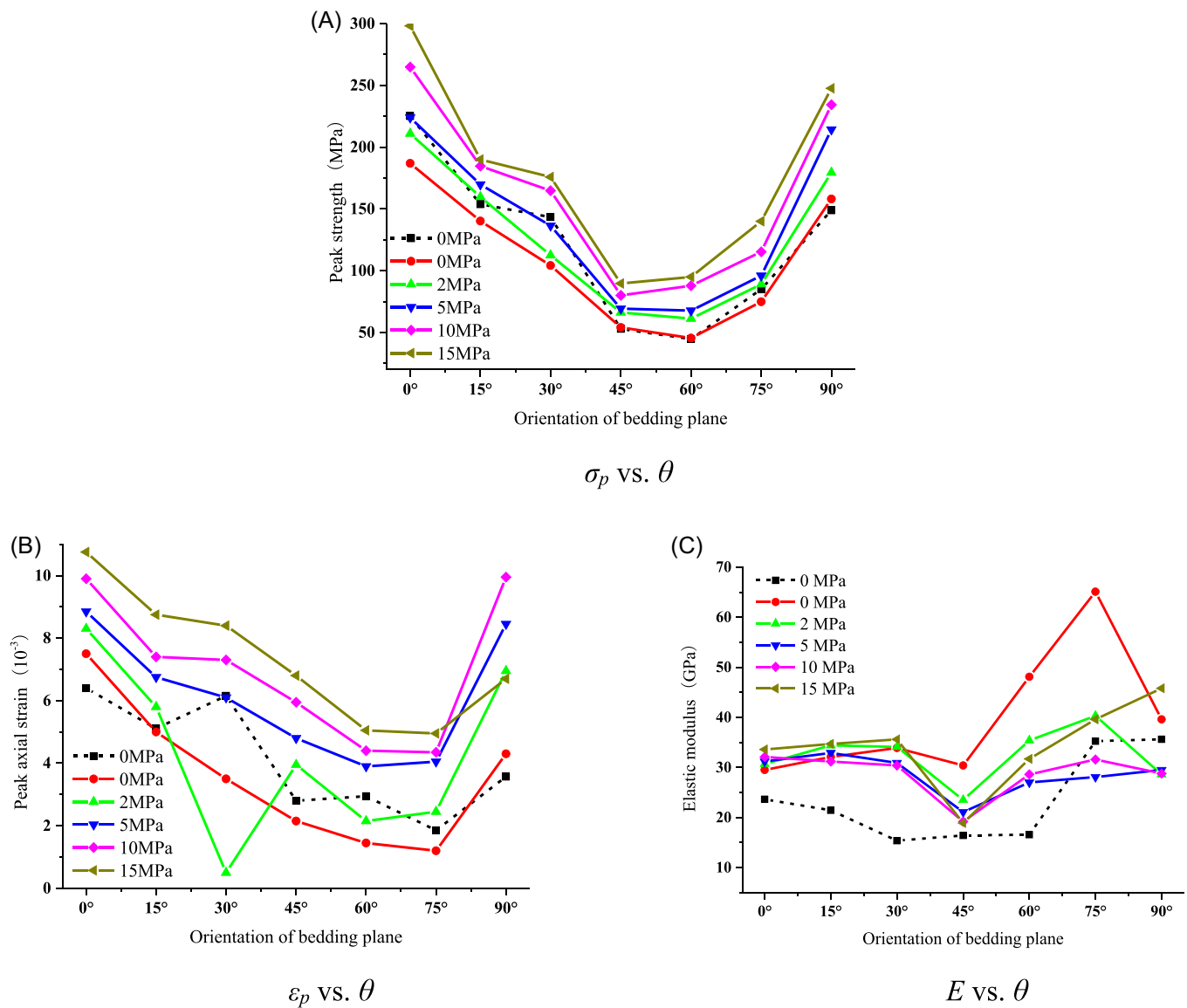


**FIGURE 9** Compressive strength ( $\sigma_p$ ), peak strain ( $\varepsilon_p$ ) and elastic modulus ( $E$ ) variation as the bedding inclination rises: (A)  $\sigma_p$  vs.  $\theta$ , (B)  $\varepsilon_p$  vs.  $\theta$  and (C)  $E$  vs.  $\theta$ .

### 3.3 | Failure modes

Figure 10 shows the failure modes of the layered rock samples under different confining pressures. When the confining pressure is 0 MPa, for the sample with an orientation of 0°, the shear failure of the rock material through the bedding surface first occurs at the middle part of the sample. With the growth of the axial load, the shear cracks gradually generate at the upper right part of the sample, and the failure mode is very similar to the laboratory test results. For the samples with the orientations of 15° and 30°, the shear failure forms at the lower and upper ends of the sample, respectively, and the failure mode was basically consistent with the laboratory test results. For the samples with the orientations of 45° and 60°, the specimen first

produces the slip failure along the bedding plane. With increasing the axial load, two parallel shear failure zones gradually appear in the specimen and intersect at a certain angle with the inclination of the bedding plane. For the samples with the orientation of 75°, the specimen mainly produces the slip failure along the bedding plane, and the failure mode is consistent with the experimental results. For the samples with the orientation of 90°, multiple splitting cracks form along the bedding plane, which is also consistent with the laboratory test results. In general, the simulated failure modes of the layered shales under uniaxial compression can be divided into three categories, that is, vertical tension-splitting failure, local slip (along bedding planes and passing rock matrix) and shear composite failure, and slip failure along the bedding plane.

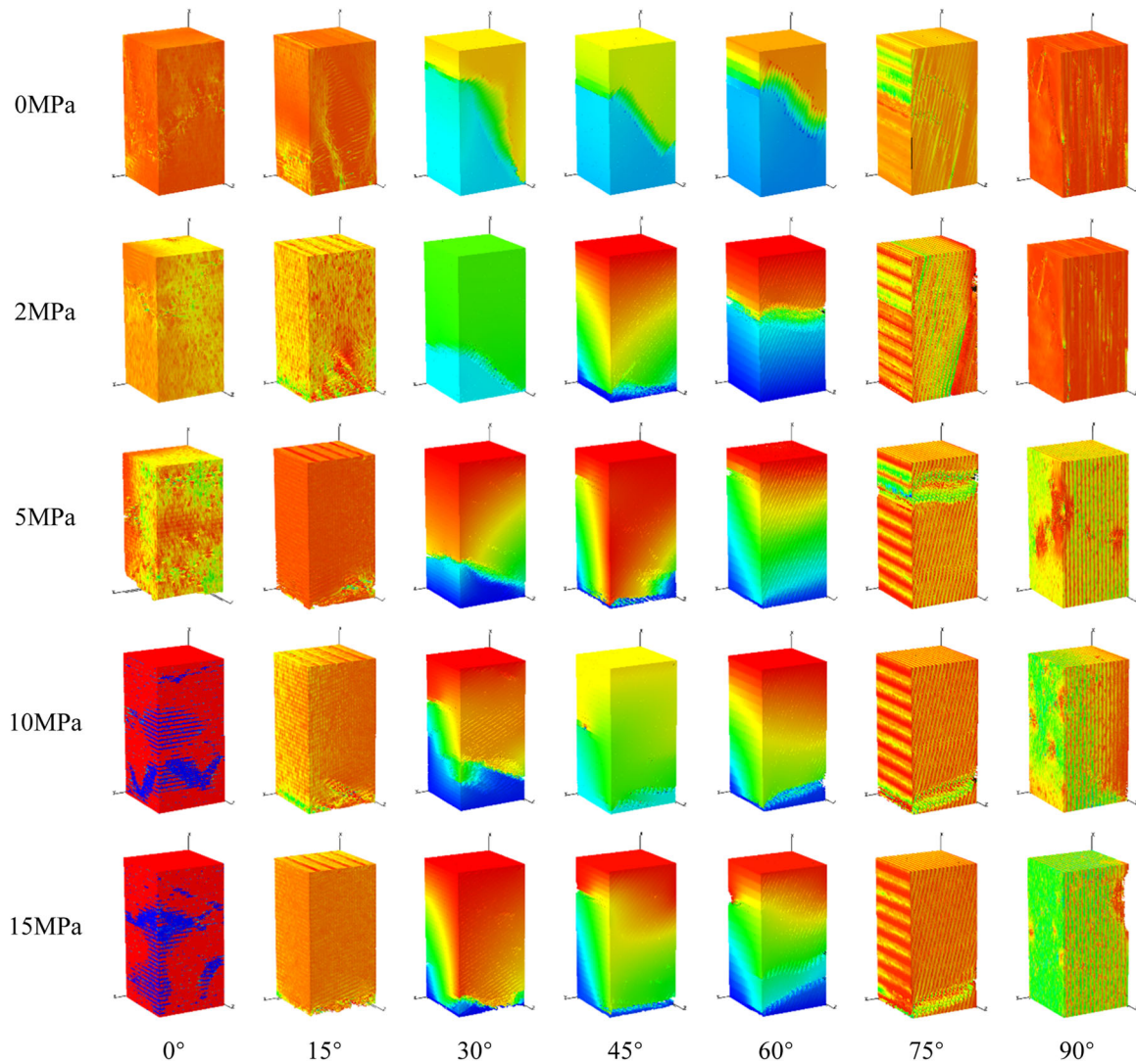


**FIGURE 10** Failure modes of layered rock specimens under different confining pressures.

With the confining pressure increasing, when the bedding plane dip angle is between  $0^\circ$  and  $30^\circ$ , the layered shale samples are mainly sheared through the bedding planes, and the failure plane and the bedding plane from a certain angle, but the cracked areas of the sample are slightly different. When the bedding plane inclination is between  $45^\circ$  and  $75^\circ$ , with the growth of the confining pressure, in addition to shear-slip failure along the bedding plane, a shear failure zone passes through the bedding plane and the slip failure gradually disappears. With the confining pressure increasing, the failure mode of the specimen gradually changes from the shear failure along bedding planes to the shear slip along the bedding planes and the shear composite failure through the bedding plane. When the bedding plane orientation is  $90^\circ$ , as the confining pressure increases, the specimen gradually changes from the vertical tension-splitting failure of the bedding planes

to the oblique shear failure of the rock material until the overall instability failure of the specimens. The failure modes of the samples under different confining pressures present various and complex characteristics.

## 4 | ESTABLISHMENT OF THE ANISOTROPIC STRENGTH CRITERION

### 4.1 | Theoretical principles

#### 1. The Jaeger strength failure criterion<sup>43</sup>

Based on the principle of a single weak plane, Jaeger<sup>43</sup> first proposed the anisotropic strength criterion that the compressive strength of transversely isotropic rock materials varies with the inclination of the bedding plane, and then it was improved by

Donath.<sup>44,45</sup> At present, the Jaeger strength criterion is widely used and the expression of the criterion is

$$\sigma_{c\theta_m} = A - D \cos 2(\theta_m - \theta_{m \min}), \quad (2)$$

where  $\theta_m$  is the angle between the maximum principal stress and the direction of the bedding plane ( $\theta_m + \theta = \frac{\pi}{2}$ ),  $\theta_{m \min}$  is the angle between the maximum principal stress and the bedding plane when the uniaxial compressive strength of the layered rock mass sample takes the minimum value, and  $A$  and  $D$  are two constants, which can be calculated according to the uniaxial compressive strength of the layered rock mass sample when  $\theta_m = 0^\circ$ ,  $30^\circ$  and  $90^\circ$ . Simultaneously, the parameter  $D$  is related to the strength anisotropy coefficient of the layered rock mass. The strength of the layered rock mass obtained by the Jaeger strength criterion varies with the inclination of the bedding plane in a 'U'-shaped curve.

## 2. The Tien-Kuo strength failure criterion<sup>46</sup>

According to the two main failure modes of layered rock samples, Tien and Kuo<sup>46</sup> proposed a transversely isotropic rock test based on the slip shear failure along the weak bedding plane and the nonslip failure of rock materials through the bedding plane. This anisotropic strength criterion is termed the Tien-Kuo strength criterion, and the expression of the criterion is:

For the nonslip shear failure mode:

$$\frac{\sigma_1(\theta_m) - \sigma_3}{\sigma_1(90^\circ) - \sigma_3} = \frac{1}{\left[ (\cos^4 \theta_m / E) + (\sin^4 \theta_m / E') + \cos^2 \theta_m \sin^2 \theta_m \left( \frac{1}{G'} - \frac{2\nu'}{E'} \right) \right] E'}, \quad (3)$$

where  $\sigma_1$  and  $\sigma_3$  are the maximum and minimum principal stresses.

The elastic modulus anisotropy coefficient of a layered rock mass  $k$  and the transverse anisotropy parameter  $n$  are defined as follows:

$$k = \frac{E}{E'}, \quad (4)$$

$$n = \frac{E'}{2G'} - \nu'. \quad (5)$$

Substituting Equations (4) and (5) into Equation (3), we can obtain

$$\frac{\sigma_1(\theta_m) - \sigma_3}{\sigma_1(90^\circ) - \sigma_3} = \frac{k}{\cos^4 \theta_m + k \sin^4 \theta_m + 2n \cos^2 \theta_m \sin^2 \theta_m}. \quad (6)$$

For the slip shear failure mode:

$$\sigma_1(\theta_m) - \sigma_3 = \frac{2(c_w + \sigma_3 \tan \varphi_w)}{(1 - \tan \varphi_w \tan \theta_m) \sin 2\theta_m}, \quad (7)$$

where  $c_w$  and  $\varphi_w$  are the cohesion and the internal friction angle of the bedding weak surface, respectively.

According to the laboratory test results of layered rock samples,  $\sigma_{1(0^\circ)}$  and  $\sigma_{1(90^\circ)}$  are usually not equal. However, in the Jaeger strength criterion, the two are assumed to be equal. To distinguish the difference between them, the Hoek-Brown criterion is used in the Tien-Kuo strength criterion to determine  $\sigma_{1(0^\circ)}$  and  $\sigma_{1(90^\circ)}$  as follows:

$$\sigma_{1(0^\circ)} - \sigma_3 = (m_{(0^\circ)} \sigma_3 \sigma_{c(0^\circ)} + \sigma_{c(0^\circ)}^2)^{0.5}, \quad (8)$$

$$\sigma_{1(90^\circ)} - \sigma_3 = (m_{(90^\circ)} \sigma_3 \sigma_{c(90^\circ)} + \sigma_{c(90^\circ)}^2)^{0.5}, \quad (9)$$

where  $\sigma_{c(0^\circ)}$  and  $\sigma_{c(90^\circ)}$  are the uniaxial compressive strengths when the bedding plane inclination  $\theta_m = 0^\circ$  and  $90^\circ$ .  $m_{(0^\circ)}$  and  $m_{(90^\circ)}$  are the parameters in the Hoek-Brown criterion corresponding to the sample with the corresponding bedding plane inclination angle, respectively.

The Tien-Kuo criterion contains seven material parameters including the cohesion and the internal friction angle of the weak bedding plane ( $c_w$  and  $\varphi_w$ ) and the rock material strength parameters ( $\sigma_{c(0^\circ)}$ ,  $\sigma_{c(90^\circ)}$ ,  $m_{(0^\circ)}$ ,  $m_{(90^\circ)}$ ,  $n$ ). The method for determining the material parameters can be found in the relevant literature Tien and Kuo.<sup>46</sup>

## 3. The improved Hoek-Brown strength criterion<sup>47</sup>

Hoek and Brown (1980)<sup>48</sup> proposed an empirical failure criterion for predicting the strength of a rock or rock mass. The expression of their criterion is

$$\sigma_1 = \sigma_3 + \sigma_{ci} \left( m \frac{\sigma_3}{\sigma_{ci}} + s \right)^\alpha, \quad (10)$$

where  $\sigma_{ci}$  is the uniaxial compressive strength of the sample and  $m$ ,  $s$  and  $\alpha$  are the material constants. When the rock is a complete rock,  $m = m_i$ ,  $s = 1$  and  $\alpha = 0.5$ .

In the Hoek-Brown criterion, the rock material parameters  $\sigma_{ci}$ ,  $m$  and  $s$  can be determined by uniaxial

and triaxial compression tests. For transversely isotropic rock samples, the sample failure is greatly affected by the inclination of the bedding planes. Hence, the Hoek–Brown criterion parameters ( $\sigma_{ci}$ ,  $m$  and  $s$ ) can also present the anisotropic characteristics. Saroglou and Tsiambaos<sup>49</sup> pointed out that the Hoek–Brown criterion parameters ( $\sigma_{ci}$ ,  $m$  and  $s$ ) were related to the intensity anisotropy coefficient  $k_\theta$ . The improved Hoek–Brown criterion can be expressed as follows:

$$\sigma_1 = \sigma_3 + \sigma_{c\theta} \left( k_\theta m_i \frac{\sigma_3}{\sigma_{c\theta}} + 1 \right)^{0.5}, \quad (11)$$

where  $\sigma_{c\theta}$  is the uniaxial compressive strength of the samples with different bedding plane inclinations  $\theta$  and  $k_\theta$  is the intensity anisotropy coefficient. If the uniaxial compression tests on samples with different bedding plane inclination angles can be carried out,  $\sigma_{c\theta}$  can be therefore determined by the test results. Saroglou and Tsiambaos<sup>49</sup> argued that the uniaxial compressive strength of layered rock samples can be determined by the Jaeger strength failure criterion by Equation (2) directly. However,  $k_\theta$  needs to be determined by a large number of uniaxial and triaxial compression tests.

#### 4. The Ramamurthy strength criterion

Ramamurthy et al.<sup>50</sup> proposed and developed a strength criterion for predicting the nonlinear strength variation characteristics of transversely isotropic rock materials, and the expression is

$$\frac{\sigma_1 - \sigma_3}{\sigma_3} = B_{\theta_m} \left( \frac{\sigma_{c\theta_m}}{\sigma_3} \right)^{\alpha_{\theta_m}}, \quad (12)$$

where  $\sigma_{c\theta_m}$  is the uniaxial compressive strength for different inclination angles  $\theta_m$  and the parameters  $B_{\theta_m}$  and  $\alpha_{\theta_m}$  can be calculated using the following equation:

$$\frac{\alpha_{\theta_m}}{\alpha_{90}} = \left( \frac{\sigma_{c\theta_m}}{\sigma_{c90}} \right)^{1-\alpha_{90}}, \quad \frac{B_{\theta_m}}{B_{90}} = \left( \frac{\alpha_{90}}{\alpha_{\theta_m}} \right)^{0.5}, \quad (13)$$

where  $\sigma_{c90}$  is the uniaxial compressive strength of the sample with the inclination  $\theta_m = 90^\circ$  and  $\alpha_{90}$  and  $B_{90}$  are the material parameters of the sample with the inclination  $\theta_m = 90^\circ$ , which can be obtained by establishing the relationship between  $\frac{\sigma_1 - \sigma_3}{\sigma_3}$  and  $\frac{\sigma_{c90}}{\sigma_3}$

through the triaxial compression test. By bringing it into Equation (13), the material parameters  $\alpha_{\theta_m}$  and  $B_{\theta_m}$  of the samples with different inclination angles  $\theta_m$  can be obtained.

#### 5. The improved Rafiai strength criterion<sup>51</sup>

Rafiai<sup>47</sup> proposed the empirical strength failure criterion for isotropic rock materials. Under triaxial compression, the expression of the strength criterion can be expressed as follows:

$$\frac{\sigma_1}{\sigma_{ci}} = \frac{\sigma_3}{\sigma_{ci}} + \left[ \frac{1 + A(\sigma_3/\sigma_{ci})}{1 + B(\sigma_3/\sigma_{ci})} \right] - r, \quad (14)$$

where  $\sigma_{ci}$  is the uniaxial compressive strength,  $A$  and  $B$  are the material constants, which depend on the mechanical properties of the rock material and  $r$  is the strength reduction factor, and for intact rock,  $r$  equals 0. For rock masses with a high degree of joint development or rock samples with many fractures,  $r$  equals 1.

For transversely isotropic rock materials, Saeidi et al.<sup>51</sup> assumed that the transversely isotropic rock material was a complete rock sample and did not consider the existence of bedding planes. Namely, they assumed  $r = 0$ . By introducing a new reduction factor that takes into account the strength anisotropy  $\alpha_\theta$ , the Rafiai strength criterion can be modified as follows:

$$\sigma_1 = \sigma_3 + \sigma_{c\theta} \left[ \frac{1 + A(\sigma_3/\sigma_{c\theta})}{\alpha_\theta + B(\sigma_3/\sigma_{c\theta})} \right], \quad (15)$$

where  $\sigma_{c\theta}$  is the uniaxial compressive strength of samples with different bedding plane inclination angles,  $\alpha_\theta$  is the strength reduction parameter related to rock anisotropy and  $A$  and  $B$  are material constants.

## 4.2 | The modified Jaeger strength criterion

### 1. Jaeger single weak surface principle

Jaeger<sup>43</sup> proposed the single weak plane principle by assuming that transversely isotropic rock material consists of rock media and a set of parallel bedding weak planes. The failure of rock media and weak bedding surface follows the Mohr–Coulomb criterion, but the cohesion and internal friction angle of rock media and weak bedding surface are not equal. Therefore, the expression of the failure criterion is:

For the destruction of rock materials:

$$\tau = c + \sigma \tan \varphi. \quad (16)$$

For the destruction of weak bedding surface:

$$\tau_\theta = c_w + \sigma_\theta \tan \varphi_w, \quad (17)$$



where  $c$  and  $\varphi$  are the cohesion and internal friction angle of rock media, respectively, and  $c_w$  and  $\varphi_w$  are the cohesion and internal friction of weak bedding plane.  $\tau$  and  $\sigma$  are the tangential stress and normal stress, respectively.  $\tau_\theta$  and  $\sigma_\theta$  are the tangential stress and normal stress when the bedding plane inclination orientation is  $\theta$ , respectively. The expression of Equation (17) in the principal stress space is

$$f(\sigma_{ij}) = (\sigma_1 - \sigma_3) - (\sigma_1 + \sigma_3)\sin\varphi - 2c\cos\varphi \quad (18)$$

$$= 0.$$

Using Equations (16) and (17), two different stress values can be obtained when the specimen fails at different bedding inclination angles, and the minimum value of the two principal stresses is treated as the failure strength of the specimen.

Figure 11 is a schematic diagram of predicting the failure strength of layered rock samples using the single weak plane principle. For the samples with the bedding orientations of  $0^\circ$  and  $90^\circ$ , the four shear strength parameters of the specimen can be determined from the triaxial compression test results. The existing laboratory test results show that the compressive strengths of the samples are not equal when the inclination angles of the bedding plane are  $0^\circ$  and  $90^\circ$ . The experimental results of the triaxial compression can be put into Equation (16) to establish the relationship between  $(\sigma_1 - \sigma_3)$  and  $(\sigma_1 + \sigma_3)$ . The cohesion and internal friction angle of the sample can be obtained by

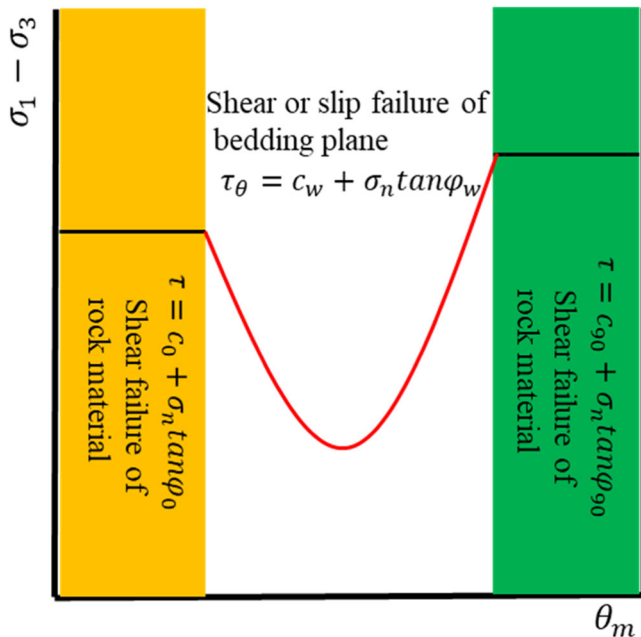


FIGURE 11 Schematic view of failure stress prediction using the single weakness plane theory.

linear fitting. It can be summarised from a large number of laboratory test results that for the layered rock mass samples when the inclination angle of the bedding plane is  $60^\circ$ , the uniaxial compressive strength of the sample reaches the minimum value, and the sample generally presents slip failure along the bedding plane. According to the triaxial compression test results, the cohesion and internal friction angle of the weak bedding plane can be obtained by fitting the results.

## 2. Modified Jaeger strength criterion

According to Jaeger's single weak plane principle, when the dip angle  $\theta$  of the layered rock sample is a middle value, the failure of the specimen is mainly the shear-slip failure of the bedding plane. However, many laboratory experiments and numerical simulations show that in addition to slip failure, there is also a small amount of shear failure of rock materials. Simultaneously, when a certain range of lateral pressure is applied, the failure mode of the specimen may change gradually, and slip failure is not the main failure mode. In this study, by introducing the anisotropic parameter  $R_{c\theta}$ , Equation (15) can be therefore modified as follows:

$$\tau_\theta = (1 + \lg R_{c\theta})c_w + \sigma_\theta \tan[(1 + \lg R_{c\theta})\varphi_w], \quad (19)$$

where  $R_{c\theta} = \frac{\sigma_{c\theta}}{\sigma_{c\min}}$  and  $\sigma_{c\min}$  is the minimum value of the uniaxial compressive strength of the layered rock mass sample, which can be obtained when the bedding orientation is  $60^\circ$ .  $\sigma_{c\theta}$  is the uniaxial compressive strength of the sample with an orientation of  $\theta$ . The expression of Equation (19) in the principal stress space can also be written as

$$\sigma_1 - \sigma_3 = (\sigma_1 + \sigma_3)\sin[(1 + \lg R_{c\theta})\varphi_w] + 2c_w \cos[(1 + \lg R_{c\theta})\varphi_w]. \quad (20)$$

Similar to Jaeger's single weak surface failure criterion, the failure of rock media and weak bedding surface can be judged by Equations (18) and (19), respectively. The determination method of the parameters  $c$ ,  $\varphi$  and  $c_w$ ,  $\varphi_w$  is consistent with the Jaeger criterion.  $\sigma_{c\theta}$  is the uniaxial compressive strength of the samples with different bedding plane inclination angles, which can be obtained by uniaxial compression test. Figure 12 shows the comparison between the results of the uniaxial compressive strength of the layered rock mass predicted by the modified Jaeger strength criterion and the experimental and numerical results, from which we can see that the theoretical prediction matches with the physical tests and numerical simulations satisfactorily.

The experimental results of shale under the conventional triaxial compression<sup>10</sup> were adopted to verify the accuracy of the modified Jaeger strength criterion under



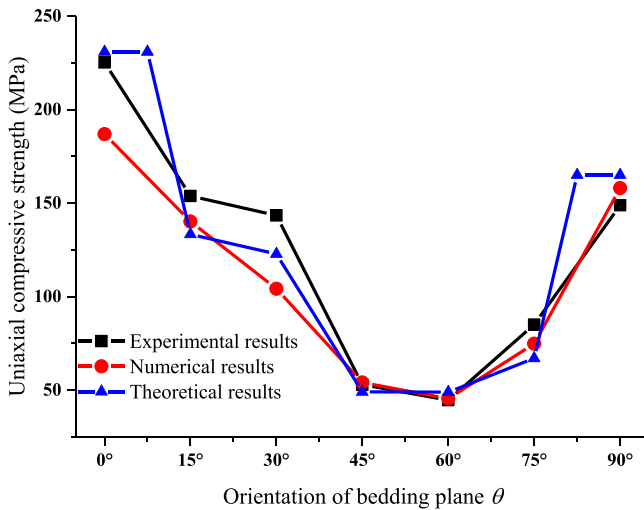


**FIGURE 12** Uniaxial compression strength predicted by the modified Jaeger strength criterion.

triaxial conditions. The parameters in the modified criterion were calculated according to the experimental data. Namely,  $c_0$ ,  $\varphi_0$ ,  $c_{90}$ ,  $\varphi_{90}$ ,  $c_w$  and  $\varphi_w$  were 28.88 MPa, 52.29°, 53.35 MPa, 45.61°, 23.96 MPa and 41.66°, respectively. When the orientation of bedding planes  $\theta$  was changed from 15° to 75°,  $R_{c\theta}$  could be obtained, respectively, based on the experimental results. The triaxial compression strengths predicted by the modified criterion and obtained by the experiments<sup>10</sup> can be seen in Figure 13. In Figure 13, the dot-dash line represents the experimental results, and the solid line represents the theoretical results. The theoretical triaxial strengths obviously show a U-shaped changing trend with increasing the orientation of bedding planes. Basically, the theoretical results are consistent with the experimental results. The comparison demonstrates that the modified Jaeger strength criterion is satisfied under triaxial conditions.

### 4.3 | Anisotropy analysis of the layered shale resistance

Nova and Sacchi<sup>52</sup> conducted a theoretical analysis on the triaxial compression of rock samples and proposed the strength failure formula of layered rock samples under the triaxial conditions. According to the uniaxial compression tests and the numerical simulations of triaxial compression, the corresponding parameters<sup>18</sup> were first determined as  $c_t = 20.03$ ,  $2\mu_t = 0.685463$ ,  $\alpha = 3.63$  and  $\beta = 0.015$  to analyse the theoretical results of the layered shales suffering triaxial compression. According to the triaxial strength failure theory, the

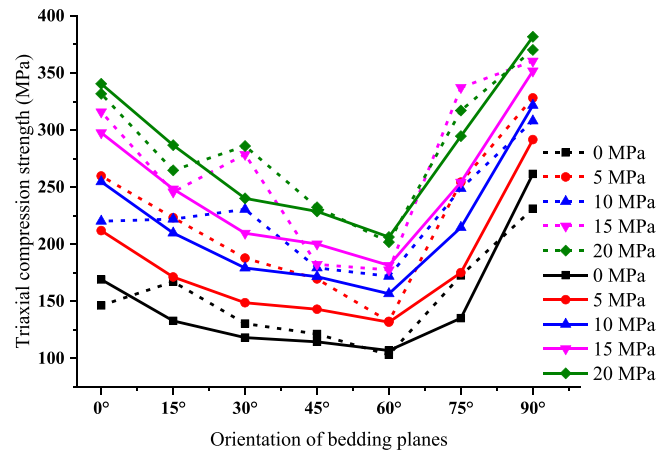


**FIGURE 13** Triaxial compression strength predicted by the modified Jaeger strength criterion.

variation law of the compressive strength of the layered rock samples under different confining pressures with the inclination of the bedding plane can be further calculated.

According to the strength theory of layered rock samples subject to triaxial conditions proposed by Nova and Sacchi,<sup>52</sup> the theoretical strength value of a layered rock mass under triaxial compression can be calculated. The results gained by the numerical simulation and theoretical prediction of triaxial compression are compared in Table 2. We can see that the variation law of the predicted results by the theory is consistent with the numerical simulation results. Simultaneously, when the inclination of the bedding plane is 30° and 90°, the compressive strength obtained from the theoretical prediction is smaller than the numerical simulation results due to the influence of the deformation localization and the progressive development of micro-cracks. The comparison of uniaxial compressive strength and triaxial compressive strength indicates that the variation law obtained by theoretical prediction analysis is more consistent with the experimental and simulated results, and the theoretical analysis is more accurate.

According to the simulated and theoretical results of triaxial compression, the changing trends of the cohesion and the internal friction angle of the layered rock samples with the inclination of the bedding plane increasing were obtained by fitting the Mohr–Coulomb criterion envelope, as shown in Figure 14. From Figure 14A, we can see that under triaxial compression, the cohesion of the shale samples obtained from the theoretical prediction and the numerical simulation first decreases and then increases with the bedding plane dip

**TABLE 2** Numerical and theoretical results of the layered rocks under triaxial compression.

$\theta$	Theoretical results (MPa)				Numerical results (MPa)			
	2 MPa	5 MPa	10 MPa	15 MPa	2 MPa	5 MPa	10 MPa	15 MPa
0°	228.88	234.27	243.21	252.05	211.00	223.95	264.94	298.18
15°	159.41	165.75	176.16	186.41	159.75	169.82	184.72	190.00
30°	97.78	104.57	115.73	126.72	112.48	136.43	164.8	175.82
45°	66.41	73.38	84.94	96.44	66.25	69.35	80.07	89.66
60°	58.13	65.37	77.42	89.47	61.20	67.65	87.85	95.01
75°	65.76	73.20	85.39	97.34	89.05	95.95	115.34	140.07
90°	81.35	88.11	99.04	109.62	179.48	214.3	234.37	247.66

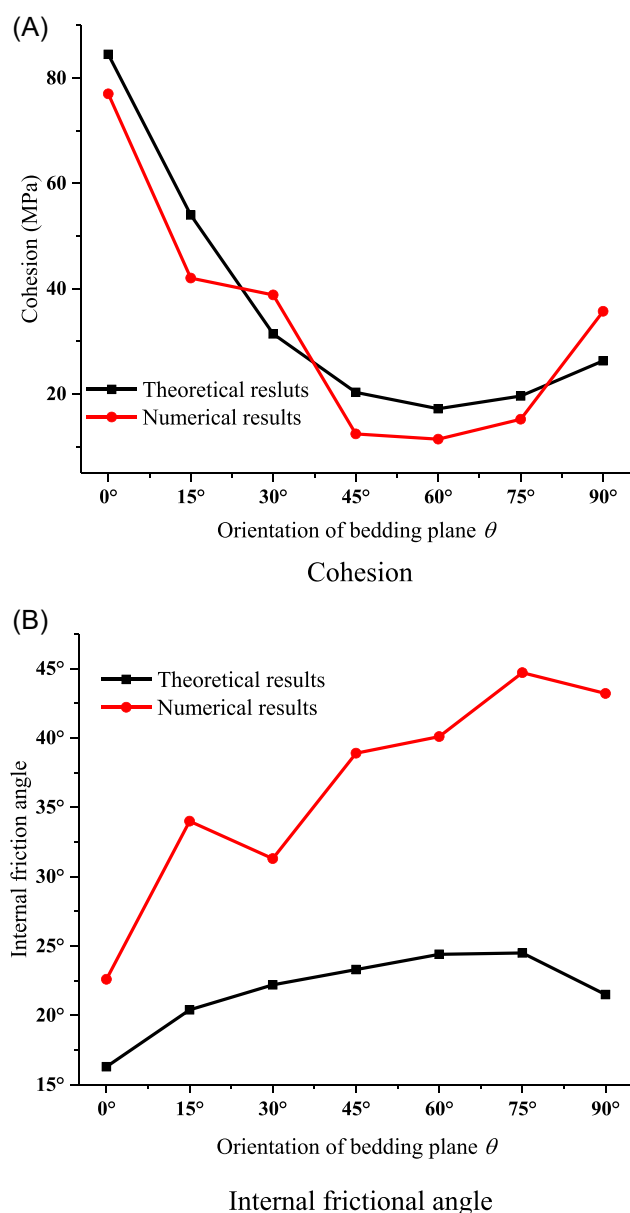


**FIGURE 14** Cohesion and internal friction angle of the layered rock specimens with different inclination angles: (A) cohesion and (B) internal friction angle

growing up, displaying a typical 'U'-shaped curve. For the cohesion, the numerical simulation results are consistent with the theoretical prediction results, and the difference between them is small. Figure 14B shows that under the condition of triaxial compression, with the inclination angle of the bedding planes increasing, the internal friction angle of the shale sample basically rises up gradually. However, the internal friction angle calculated by the theoretical prediction is smaller than the numerical simulation because the gradual creation and propagation of microcracks cannot be considered in the theoretical prediction.

## 5 | CONCLUSION

In this study, to improve our understanding of the effect of bedding surfaces on the anisotropic deformation and strength parameters of layered shales, systemic numerical simulations and theoretical analyses were conducted. The progressive failure process of layered shales was modelled based on the statistical strength theory, damage mechanics and continuum theory. Furthermore, the influence of the formation and development of microcracks on the mechanical resistance and failure mode of layered shales was comprehensively discussed. Besides, the modified Jaeger strength criterion was proposed. The main conclusions can be drawn as follows:

1. As the inclination angle of the bedding planes grows up, the compressive strength of the layered shales first decreases and then increases, showing a typical 'U'-shaped variation. For the layered rock samples with the same bedding orientation, the compressive strength increases gradually with the growth of the confining pressure. Furthermore, when the bedding plane inclination is 0°, the peak intensity of the sample is the largest, and when the inclination of the bedding plane is 45° or 60°, the peak intensity of the sample is the smallest.

2. With the inclination angle of the bedding planes rising, the variation of the axial strain value at the peak point is similar to the compressive strength, that is, the typical 'U'-shaped changing trend. When the confining pressure is 2 MPa, the strain value at the peak point fluctuates slightly, but the variation law is basically consistent with the other confining pressures. Meanwhile, with the inclination angle of the bedding planes increasing, the elastic modulus first decreases, later increases and then decreases, showing the 'W'-shaped curve. When the inclination of the bedding planes is 30° or 75°, the elastic modulus reaches the peak point. However, the elastic modulus reaches the minimum value when the bedding plane inclination angle is 45°.
3. The simulated failure modes of the layered shales under uniaxial compression can be divided into three categories, that is, the vertical tension-splitting failure, the local slip (along bedding planes and passing rock matrix) and shear composite failure, and the slip failure along bedding planes. When the bedding plane dip angle is between 0° and 30°, the layered shale samples are mainly sheared through the bedding planes. When the bedding plane inclination is between 45° and 75°, a shear failure zone passes through the bedding planes, and the slip failure gradually disappears. When the bedding plane orientation is 90°, as the confining pressure increases, the specimen gradually changes from the vertical tensile splitting failure of the bedding planes to the oblique shear failure of the rock media.
4. The modified Jaeger strength criterion was proposed by introducing the anisotropic parameter  $R_{\theta}$ . The modified Jaeger strength criterion was verified by the numerical and experimental results. It can reflect the failure mode and strength characteristics of layered rock masses to a certain extent. Under the triaxial compression conditions, with the inclination angle of the bedding planes growing up, the cohesion of the layered shale sample first decreases and then increases, showing a typical 'U'-shaped variation, while the internal friction angle of the layered shale sample gradually increases.

## AUTHOR CONTRIBUTIONS

**Min Gao:** Investigation; formal analysis; data curation; funding acquisition; writing—original draft. **Bin Gong:** Conceptualization; methodology; supervision; writing—review and editing. **Zhengzhao Liang:** Supervision, writing—review and editing. **Shanpo Jia:** Methodology; writing—review and editing. **Jiuqun Zou:** Validation; visualization.

## ACKNOWLEDGEMENTS

The authors appreciate the financial support by the Natural Science Research Project of Anhui University (Grant No. 2022AH050798), the Anhui Provincial Natural Science Foundation, China (Grant No. 2108085QE208), the Scientific Research Foundation for High-level Talents of Anhui University of Science and Technology, the China Postdoctoral Science Foundation (Grant No. 2021M700753), the Open Project Funded by the Engineering Research Center of Underground Mine Construction, Ministry of Education, China (Grant No. JYBGCZX2022108) and the University Synergy Innovation Programme of Anhui Province, China (Grant No. GXXT-2022-20).

## CONFLICT OF INTEREST STATEMENT

The authors declare no conflict of interest.

## DATA AVAILABILITY STATEMENT

The data sets generated and/or analysed during the current study are available from the corresponding author upon request.

## ORCID

Bin Gong  <http://orcid.org/0000-0002-9464-3423>

Shanpo Jia  <http://orcid.org/0000-0002-7841-6239>

## REFERENCES

1. Yang J, Fan P, Wang M, Li J, Dong L. Experimental study on the irreversible displacement evolution and energy dissipation characteristics of disturbance instability of regular joints. *Deep Undergr Sci Eng.* 2023;2(1):20-36.
2. Zhang C, Zhu Z, Wang S, Ren X, Shi C. Stress wave propagation and incompatible deformation mechanisms in rock discontinuity interfaces in deep-buried tunnels. *Deep Undergr Sci Eng.* 2022;1(1):25-39.
3. Wang Z, Pan PZ, Liu X, Zhou Y, Hou W, Yang S. A hybrid anisotropic elastoplastic model for layered rock mass and numerical implementation. *Int J Geomech.* 2023;23(4):04023019.
4. Feng XH, Gong B, Cheng XF, Zhang HH, Tang CA. Anisotropy and microcrack-induced failure precursor of shales under dynamic splitting. *Geomat Nat Hazards Risk.* 2022;13(1):2864-2889.
5. Wang YY, Gong B, Tang CA. Numerical investigation on anisotropy and shape effect of mechanical properties of columnar jointed basalts containing transverse joints. *Rock Mech Rock Eng.* 2022;55:7191-7222.
6. Wang Y, Gong B, Tang C, Zhao T. Numerical study on size effect and anisotropy of columnar jointed basalts under uniaxial compression. *Bull Eng Geol Environ.* 2022;81:41.
7. Wu N, Liang ZZ, Li YC, Qian XK, Gong B. Effect of confining stress on representative elementary volume of jointed rock masses. *Geomech Eng.* 2019;18(6):627-638.
8. Yin PF, Yang SQ, Gao F, Tian WL. Experiment and DEM simulation study on mechanical behaviors of shale under

- triaxial cyclic loading and unloading conditions. *Geomech Geophys Geo-Energy Geo-Resour.* 2023;9:10.
9. Jin ZF, Li WX, Jin CR, Hambleton J, Cusatis G. Anisotropic elastic, strength, and fracture properties of Marcellus shale. *Int J Rock Mech Min Sci.* 2018;109:124-137.
  10. Yang SQ, Yin PF, Ranjith PG. Experimental study on mechanical behavior and brittleness characteristics of Longmaxi formation shale in Changning, Sichuan Basin, China. *Rock Mech Rock Eng.* 2020;53:2461-2483.
  11. Mandal PP, Sarout J, Rezaee R. Triaxial deformation of the Goldwyer gas shale at in situ stress conditions—part I: anisotropy of elastic and mechanical properties. *Rock Mech Rock Eng.* 2022;55:6121-6149.
  12. Li D, Wong LNY, Liu G, Zhang X. Influence of water content and anisotropy on the strength and deformability of low porosity meta-sedimentary rocks under triaxial compression. *Eng Geol.* 2012;126:46-66.
  13. Liao AJ, Meng LB, Li TB, Lu Q, Cheng W. Experimental study on anisotropic layered sandstone under the thermal-mechanical action. *Chin J Rock Mech Eng.* 2019;38(S1):2593-2592.
  14. Li DY, Qiu JD, Li XB. Experimental study on dynamic tensile and compressive properties of bedding sandstone under impact loading. *Chin J Rock Mech Eng.* 2015;34(10):2091-2097.
  15. Li ZG, Xu GL, Huang P, Zhao X, Fu YP, Su C. Mechanical and anisotropic properties of silty slates. *Rock Soil Mech.* 2018;39(5):200-209.
  16. Gholami R, Rasouli V. Mechanical and elastic properties of transversely isotropic slate. *Rock Mech Rock Eng.* 2014;47(5):1763-1773.
  17. Tien YM, Tsao PF. Preparation and mechanical properties of artificial transversely isotropic rock. *Int J Rock Mech Min Sci.* 2000;37(6):1001-1012.
  18. Nova R. The failure of transversely isotropic rocks in triaxial compression. *Int J Rock Mech Min Sci Geomech Abstr.* 1980;17(6):325-332.
  19. Hakala M, Kuula H, Hudson JA. Estimating the transversely isotropic elastic intact rock properties for in situ stress measurement data reduction: a case study of the Olkiluoto mica gneiss, Finland. *Int J Rock Mech Min Sci.* 2007;44(1):14-46.
  20. Zhou YY, Feng XT, Xu DP, Fan QX. Experimental investigation of the mechanical behavior of bedded rocks and its implication for high sidewall caverns. *Rock Mech Rock Eng.* 2016;49(9):3643-3669.
  21. Wang Z, Zhang Q, Liu J, Fu LY. Effective moduli of rocks predicted by the Kuster-Toksöz and Mori-Tanaka models. *J Geophys Eng.* 2021;18:539-557.
  22. Dambly MLT, Nejati M, Vogler D, Saar MO. On the direct measurement of shear moduli in transversely isotropic rocks using the uniaxial compression test. *Int J Rock Mech Min Sci.* 2019;113:220-240.
  23. Gonzaga GG, Leite MH, Corthésy R. Determination of anisotropic deformability parameters from a single standard rock specimen. *Int J Rock Mech Min Sci.* 2008;45(8):1420-1438.
  24. Cho JW, Kim H, Jeon S, Min KB. Deformation and strength anisotropy of Asan gneiss, Boryeong shale, and Yeoncheon schist. *Int J Rock Mech Min Sci.* 2012;50:158-169.
  25. Togashi Y, Kikumoto M, Tani K, Hosoda K, Ogawa K. Detection of deformation anisotropy of tuff by a single triaxial test on a single specimen. *Int J Rock Mech Min Sci.* 2018;108:23-36.
  26. Togashi Y, Kikumoto M, Tani K. An experimental method to determine the elastic properties of transversely isotropic rocks by a single triaxial test. *Rock Mech Rock Eng.* 2016;50(1):1-15.
  27. Debecker B, Vervoort A. Two-dimensional discrete element simulations of the fracture behavior of slate. *Int J Rock Mech Min Sci.* 2013;61(61):161-170.
  28. Liang ZZ, Tang CA, Li HX, Xu T, Yang TH. A numerical study on failure process of transversely isotropic rock subjected to uniaxial compression. *Rock Soil Mech.* 2005;26(1):57-62.
  29. Xia L, Zeng YW, Zhang S. Influence of meso-mechanical parameters of bedding plane on strength characteristics of layered rock mass. *J Yangtze River Sci Res Inst.* 2016;33(7):68-75. (in Chinese)
  30. Shen B, Shi J, Rinne M, et al. Two-dimensional displacement discontinuity method for transversely isotropic materials. *Int J Rock Mech Min Sci.* 2016;83:218-230.
  31. Park B, Min KB, Thompson N, Horsrud P. Three-dimensional bonded-particle discrete element modeling of mechanical behavior of transversely isotropic rock. *Int J Rock Mech Min Sci.* 2018;110:120-132.
  32. Lisjak A, Tatone BSA, Grasselli G, Vietor T. Numerical modelling of the anisotropic mechanical behaviour of Opalinus clay at the laboratory-scale using FEM/DEM. *Rock Mech Rock Eng.* 2014;47(1):187-206.
  33. Chen TT, Foulger GR, Tang CA, Mathias SA, Gong B. Numerical investigation on origin and evolution of polygonal cracks on rock surfaces. *Eng Geol.* 2022;311:106913.
  34. Gong B, Tang CA, Wang SY, Bai HM, Li YC. Simulation of the nonlinear mechanical behaviors of jointed rock masses based on the improved discontinuous deformation and displacement method. *Int J Rock Mech Min Sci.* 2019;122:104076.
  35. Wang Y, Gong B, Tang C. Numerical investigation on fracture mechanisms and energy evolution characteristics of columnar jointed basalts with different model boundaries and confining pressures. *Front Earth Sci.* 2021;9:763801.
  36. Gong B, Wang YY, Zhao T, Tang CA, Yang XY, Chen TT. AE energy evolution during CJB fracture affected by rock heterogeneity and column irregularity under lateral pressure. *Geomat Nat Hazards Risk.* 2022;13(1):877-907.
  37. Wang Y, Gong B, Zhang Y, Yang X, Tang C. Progressive fracture behavior and acoustic emission release of CJBs affected by joint distance ratio. *Mathematics.* 2022;10:4149.
  38. Yu C, Gong B, Wu N, Xu P, Bao X. Simulation of the fracturing process of inclusions embedded in rock matrix under compression. *Appl Sci.* 2022;12(16):8041.
  39. Chen B, Gong B, Wang S, Tang C. Research on zonal disintegration characteristics and failure mechanisms of deep tunnel in jointed rock mass with strength reduction method. *Mathematics.* 2022;10(6):922.
  40. Gong B, Wang S, Sloan SW, Sheng D, Tang C. Modelling rock failure with a novel continuous to discontinuous method. *Rock Mech Rock Eng.* 2019;52:3183-3195.
  41. Gong B, Liang ZZ, Liu XX. Nonlinear deformation and failure characteristics of horseshoe-shaped tunnel under varying principal stress direction. *Arab J Geosci.* 2022;15:475.

42. Tang CA. Numerical simulation of progressive rock failure and associated seismicity. *Int J Rock Mech Min Sci.* 1997;34(2):249-261.
43. Jaeger JC. Shear failure of anisotropic rocks. *Geol Mag.* 1960;97(1):65-72.
44. Donath FA. Experimental study of shear failure in anisotropic rocks. *Geol Soc Am Bull.* 1961;72(6):985-989.
45. Donath FA. Strength variation and deformational behavior in anisotropic rock. In: Judd JW, ed. *State of Stress in the Earth's Crust.* Elsevier; 1964:281-300.
46. Tien YM, Kuo MC. A failure criterion for transversely isotropic rocks. *Int J Rock Mech Min Sci.* 2001;38(3): 399-412.
47. Rafiai H. New empirical polyaxial criterion for rock strength. *Int J Rock Mech Min Sci.* 2011;48(6):922-931.
48. Hoek E, Brown ET. *Underground excavations in rock.* Taylor & Francis Group; 1980.
49. Saroglou H, Tsiambaos G. A modified Hoek–Brown failure criterion for anisotropic intact rock. *Int J Rock Mech Min Sci.* 2008;45(2):223-234.
50. Ramamurthy T, Rao GV, Singh J. A strength criterion for transversely isotropic rocks. In: *Proceeding of the Fifth Australia-New Zealand Conference on Geomechanics, Sydney, Australia*, Vol 1. 1988:253-257.
51. Saeidi O, Rasouli V, Vaneghi RG, Gholami R, Torabi SR. A modified failure criterion for transversely isotropic rocks. *Geosci Front.* 2014;5(2):215-225.
52. Nova R, Sacchi G. A generalized failure condition for orthotropic solids. In: Boehler JP, ed. *Proceeding of EUROMECH 115, CNRS International Colloquium 'Mechanical Behavior of Anisotropic Solids', Grenoble, France*, Springer, Dordrecht; 1982.

**How to cite this article:** Gao M, Gong B, Liang Z, Jia S, Zou J. Investigation of the anisotropic mechanical response of layered shales. *Energy Sci Eng.* 2023;1-18. doi:10.1002/ese3.1611